Analytic, nonlinearly exact solutions for an rf confined plasma

Kushal Shah and Harishankar Ramachandran

Citation: Phys. Plasmas **15**, 062303 (2008); doi: 10.1063/1.2926632
View online: http://dx.doi.org/10.1063/1.2926632
View Table of Contents: http://pop.aip.org/resource/1/PHPAEN/v15/i6
Published by the American Institute of Physics.

Analytic, nonlinearly exact solutions for an rf confined plasma

Kushal Shah[a] and Harishankar Ramachandran[b]
Department of Electrical Engineering, IIT Madras, Chennai-600036, India

(Received 31 December 2007; accepted 22 April 2008; published online 6 June 2008)

RF confined electron plasmas are of importance in Paul traps [W. Paul, Rev. Mod. Phys. **62**, 531 (1990)]. The stability of such plasmas is unclear and statistical heating arguments have been advanced to explain the observed heating in such plasmas [I. Siemers *et al.*, Phys. Rev. A **38**, 5121 (1988)]. This study investigates the nature of a one-dimensional collisionless electron plasma that is confined by an rf field of the form $[-B+A\cos(\omega t)]x$, where x is the space coordinate and ω is the rf frequency. Nonlinearly exact solutions are obtained. The distribution function and the plasma density are obtained in closed form and have constant shapes with time varying oscillations. These oscillations are at the rf frequency and its harmonics, modulated by a low frequency related to the electron bounce time. The linear limit of weak fields is recovered. Analytic expressions are obtained for the required external field to make it consistent with prescribed distribution functions. These solutions remain valid even in the presence of collisions. Solutions involving multiple species are also obtained, though only for collisionless traps. It is found that the ponderomotive force response needs to be corrected to account for the temperature fluctuations. No stochastic heating is observed in this field configuration. © *2008 American Institute of Physics*. [DOI: 10.1063/1.2926632]

I. INTRODUCTION

Interactions of plasmas with rf waves have been extensively studied in connection with Paul traps.[1] RF confinement of plasmas has also been a topic of immense interest.[2–8]

To explain the interaction of rf waves with plasma, statistical arguments have been offered.[9–13] There are two kinds of stochastic approaches. One is to consider the plasma behavior as a consequence of Brownian motion[9] and the other is the idea of Fermi acceleration.[11,12] In the Brownian motion approach, the motion of the electrons is assumed random, and approximate expressions for the density and distribution functions are derived using probabilistic arguments. In the case where Fermi acceleration[14] is considered, the rf field is assumed to die down very quickly with distance inside the plasma boundary, thus forming a reflecting structure resembling a wall and electrons are reflected off this "wall" resulting in the heating of their distribution. These wall-like structures near the plasma boundary are called rf sheaths and their characteristics have been well studied.[15–18] As these reflected electrons return to the bulk of the plasma, they transfer their energy to the bulk plasma by undergoing collisions, which results in the heating up of the plasma as a whole.

Although these models are quite promising, it is not clear if they resemble plasma behavior completely in all its aspects. The Brownian motion model requires the plasma to be highly collisional, which rules out analysis of collisionless plasmas. The Fermi acceleration model is for capacitive discharges, where the plasma is assumed to be collisionless[19] near the plasma boundary and accounts for the heating of electrons due to fields which are localized within a sheath of marginal thickness near the plasma boundary.

There is, also, a third category of solutions which attempt to solve the collisionless Vlasov equation. In these attempts (Krapchev and Abhay[20,21]), it is assumed that the time-varying distribution function can be decomposed as a Fourier series which has the same period as the rf wave. Under this assumption, the Vlasov equation is then solved to obtain expressions for the time averaged distribution function and density.

In addition to these studies on plasmas confined by rf fields, there have also been many investigations into the nature of rf-induced wave phenomena in plasmas.[22,23]

This paper analyzes the problem of an electron plasma confined partly by rf and partly by static potentials. Pure rf confinement and purely static confinement are valid limits of this analysis. A very specific form of the total electric field is considered that leads to tractable equations. The analysis is for a one-dimensional collisionless pure electron plasma with a nonuniform electrostatic standing wave. The field is assumed to be given by

$$E(x,t) = -\frac{m}{e}[-B + A\cos(\omega t)]x, \tag{1}$$

where A, B are constants, w is the rf frequency, and m and $-e$ are the mass and charge of an electron, respectively. Exact solutions are obtained for arbitrary initial conditions. Conventionally, plasma response to fields of the kind as in Eq. (1) for $B=0$ is covered under the notion of the "ponderomotive effect." To interpret the results obtained in this paper, we compare them with conventional ponderomotive force theory, which is briefly discussed below, and the linear Vlasov theory.

The ponderomotive effect[24–31] describes the response of a plasma to fields of the form $E(x,t)=g(x)\cos(wt)$. Particles under a force of this form are pushed away from high field regions and a drift motion is superimposed on the high fre-

[a]Electronic mail: atmabodha@gmail.com.
[b]Electronic mail: hsr@ee.iitm.ac.in.

quency response. The force equation for an electron in such a field is given by

$$\frac{d^2x}{dt^2} = -\frac{e}{m}g(x)\cos(wt).$$

We divide the path of the particle, $x(t)$, into two components $x(t)=x_0(t)+x_1(t)$, where x_0 represents the drift and x_1 represents the high frequency component. Now, Taylor expanding $g(x)$ about x_0, we get

$$\frac{d^2x_0}{dt^2} + \frac{d^2x_1}{dt^2} = -\frac{e}{m}\left[g(x_0) + \left.\frac{dg}{dx}\right|_{x_0} x_1\right]\cos(wt),$$

where terms of order $O[g''(x_0)x_1^2]$ are neglected and it is assumed that x_1 is small compared to the scale length of the spatial variation of $g(x)$. If we average the above equation over the fast time scale, we obtain

$$\left\langle \frac{d^2x_0}{dt^2} \right\rangle = -\left.\frac{e}{m}\frac{dg}{dx}\right|_{x_0} \langle x_1 \cos(wt)\rangle,$$

where $\langle..\rangle$ represents average over the fast time scale. The remaining part of the equation is

$$\frac{d^2x_1}{dt^2} = -\frac{e}{m}g(x_0)\cos(wt),$$

where $x_0''-\langle x_0''\rangle$ and $[-eg'(x_0)/m][x_1\cos(wt)-\langle x_1\cos(wt)\rangle]$ have been neglected as small.

This equation can be easily solved to give

$$x_1 = \frac{e}{mw^2}g(x_0)\cos(wt).$$

Substituting this in the equation for x_0 and averaging over the fast time scale, we obtain

$$\frac{d^2x_0}{dt^2} = -\left.\frac{e^2}{4m^2w^2}\frac{d}{dx}g^2(x)\right|_{x_0} \tag{2}$$

which is the well-known ponderomotive force equation. The above derivation is valid if x_1 is small compared to the scale length of spatial variation of $g(x)$. For this to be true, the spatial gradient of the field must be small.

It is also widely accepted that the time-averaged density of the electrons in the plasma under an electric field of the form $E(x,t)=g(x)\cos(wt)$ is given by

$$n(x) = n_0 \exp\left(-\frac{\phi_P}{kT}\right), \tag{3}$$

where n_0 is the electron density in the absence of the electric field and ϕ_P is the fictitious ponderomotive potential given by

$$\phi_P(x) = \frac{e^2}{4m^2w^2}g^2(x).$$

This result was formally derived from kinetic theory by Krapchev.[20]

In the following sections, we analyze the response of a plasma to the electric field of Eq. (1). Exact solutions of the kinetic equations are obtained. This paper has been organized as follows: In Sec. II, we solve the equation of motion of the electron under an electric field as given in Eq. (1) and obtain closed form solutions for the path of the electron at any future time for arbitrary initial conditions. Then, in Sec. III, we derive closed form analytic expressions for the time evolution of the distribution function and density of the plasma under this force field. Then in Sec. IV, we use the expressions found in Secs. II and III to obtain a self-consistent model of the plasma. Section V is devoted to some discussion on the results found and Sec. VI contains conclusions. Appendices A–D, in the EPAPS,[41] contain the derivations of some of the results presented in this paper.

II. THE EQUATIONS OF MOTION

Consider an electric field given in Eq. (1). It must be noted that this total electric field does not satisfy the Poisson's equation because $\partial E/\partial x \neq \rho/\epsilon_0$. Thus, the solution is only valid if the electric field has gradients along $\hat{y}$ and $\hat{z}$. Such a field would cause particle flow along all three directions unless there were some means of constraining particle motion along $\hat{x}$ such as the presence of a strong magnetic field. This limits the extent to which the solutions in this paper are "self-consistent."

The force equation for an electron under this field is

$$\frac{d^2x}{dt^2} = [-B + A\cos(wt)]x. \tag{4}$$

By transforming to $z=\exp(jwt)$, Eq. (4) becomes a linear differential equation whose coefficients are polynomials in z. In previous treatments for the case when $B=0$, this has led to the assumption that under the effect of this force field, the time evolution of the distribution function of the plasma is a power series in z, i.e., expressible as a Fourier series in time with fundamental frequency w (Refs. 20 and 21). Unfortunately, this is not the case as the solution is actually a generalized power series in $\exp(jwt)$ and a new frequency, ν, appears. This new frequency contains the ponderomotive effect.

We make a transformation of variables, $\tau=wt/2$, writing $2A/w^2$ as q and $4B/w^2$ as p to get

$$\frac{d^2x}{d\tau^2} = [-p + 2q\cos(2\tau)]x. \tag{5}$$

Equation (5) is the Mathieu's equation[32] whose solutions are well known. This equation does not have stable solutions for all p,q. For a given q, there are values of p denoted by $a_0,a_1,a_2,\ldots$, for which Eq. (5) has even periodic solutions

and there are also other values of p denoted by $b_1, b_2, \ldots$. for which the equation has odd periodic solution. These two sets of values $(a_0, a_1, a_2, \ldots)$ and $(b_1, b_2, \ldots)$ form two countably infinite sets and are called the characteristic values. If q is real, the characteristic values a_r and b_r are also real and are distinct. For $q>0$, we have $a_0<b_1<a_1<b_2<\ldots$. For $p=0$, the solutions are stable if $0 \leqslant q \leqslant q_c$, where $q_c \approx 0.9$. This corresponds to the case when the particles see only the rf field. If $p<0$, then the dc field is trying to throw away the electrons to infinity. For this case, any arbitrarily small positive value of q will not be sufficient to confine the plasma. Thus, when $p<0$, there is both a nonzero positive lower bound and an upper bound on the value of q for the solutions of Eq. (5) to be stable. This corresponds to the case when the total dc field is trying to destabilize the plasma but the rf field comes in and makes the particle orbits bounded and hence stable. For $p>0$, both the dc and the rf field contribute towards confining the plasma.

Mathieu's equations have been used before[1] to analyze plasma dynamics in Paul traps. However, the analysis was restricted to finding the stability boundary. In another paper,[33] Mathieu's equations were used to study stochastic heating of orbits in the presence of large amplitude standing waves. The analysis was, however, not carried forward to obtain time evolution expressions for the distribution function and density of the plasma.

Equation (5) has two linearly independent solutions,[34,35] $\phi(\tau)$ and $\psi(\tau)$, which are given by

$$\phi(\tau) = \sum_{r=-\infty}^{\infty} c_{2r} \cos[(\nu + 2r)\tau] \tag{6}$$

and

$$\psi(\tau) = \sum_{r=-\infty}^{\infty} c_{2r} \sin[(\nu + 2r)\tau], \tag{7}$$

where c_{2r} for $r=0, \pm 1, \pm 2, \ldots$ are constant coefficients related by the following recurrence relation:

$$[p - (\nu + 2r)^2]c_{2r} = q(c_{2r-2} + c_{2r+2}) \tag{8}$$

and ν is given as the solution of an asymptotic series,

$$p = \nu^2 + \frac{1}{2(\nu^2-1)}q^2 + \frac{5\nu^2+7}{32(\nu^2-1)^3(\nu^2-4)}q^4 + \frac{9\nu^4+58\nu^2+29}{64(\nu^2-1)^5(\nu^2-4)(\nu^2-9)}q^6 + O(q^8). \tag{9}$$

For $p, q \ll 1$, we can approximately solve Eq. (9) to get

$$\nu \approx \sqrt{p + \frac{q^2}{2}}. \tag{10}$$

As an example, consider the case of $q=0.16$ and $p=-0.01$. This case corresponds to a field given by

$$E(x,\tau) = -(m/e)[-0.01 + 0.32\cos(2\tau)]x.$$

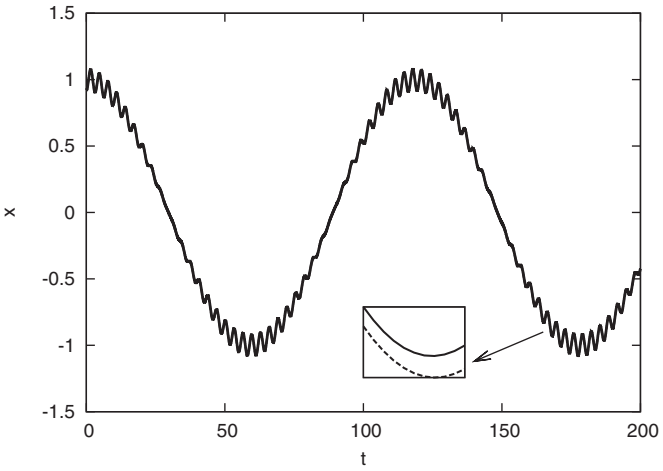

FIG. 1. The solid line shows the plot of the path of the particle as per numerical integration of Eq. (5). The dashed line shows the path as predicted by the mathematical expression given in Eq. (11), considering only the first three terms. This was done for $q=0.16$, $p=-0.01$, and the initial conditions are $x_0=0.91918$, $v_0=0$. We can see that there is close agreement between mathematics and simulation and little discrepancy can be reduced further by considering higher order terms in the mathematical expression.

The high frequency response should be roughly $\delta x \approx -0.08 x_0 \cos(2\tau)$. Thus, this is a regime where $|\delta x| \ll |x_0|$, as required for conventional ponderomotive theory to be valid. For this case, the expressions for ϕ and ψ are

$$\begin{aligned}\phi(\tau) &\approx \cos(\nu\tau) - 0.03789\cos(\nu+2)\tau \\ &\quad - 0.04211\cos(\nu-2)\tau + 0.0003688\cos(\nu+4)\tau \\ &\quad + 0.0004322\cos(\nu-4)\tau, \\ \psi(\tau) &\approx \sin(\nu\tau) - 0.03789\sin(\nu+2)\tau \\ &\quad - 0.04211\sin(\nu-2)\tau + 0.0003688\sin(\nu+4)\tau \\ &\quad + 0.0004322\sin(\nu-4)\tau,\end{aligned} \tag{11}$$

where $\nu=0.0529$.

The solid line in Fig. 1 displays the plot of the numerical solution of Eq. (5) for $q=0.16$, $p=-0.01$ and initial conditions $x_0=0.91918, v_0=0$. The dashed line is the analytic solution as given in Eq. (11) considering the first three terms. This reveals the simple structure lying behind these complex looking orbits. There is a small mismatch between the two plots which is due to the fact that the full analytic solution contains an infinite number of terms and accuracy can be improved by including more terms in the expression. This regime is clearly one where the δx due to the high frequency wave is small compared to the distance between turning points. The phase space plot for this case is shown in Fig. 2. When q becomes large, $|\delta x| \sim |x_0|$ and the assumptions leading to the derivation of the ponderomotive force expression become invalid.

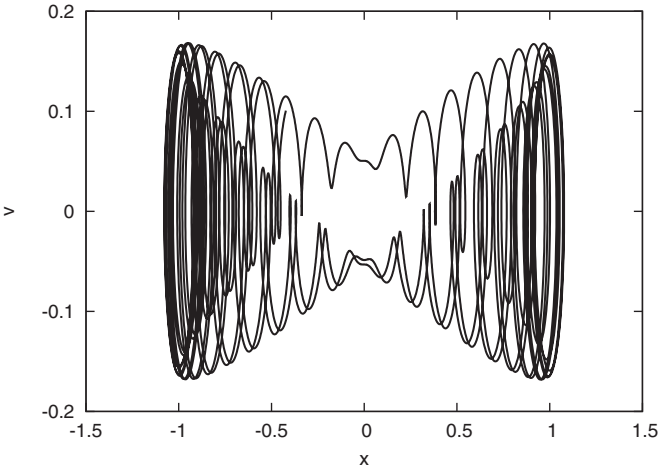

FIG. 2. This is the phase space plot of the trajectory shown in Fig. 1. We can see that near $x=1$ and $x=-1$, the particle is undergoing high frequency oscillations. This is the region of phase space for which the ponderomotive theory holds.

The general solution to Eq. (5) is

$$x(\tau) = D\phi(\tau) + E\psi(\tau), \tag{12}$$

where D and E are constants that depend on the initial conditions, namely the particle position and velocity at $\tau=0$.

As can be seen in Eq. (11), the coefficients in the expression for ϕ and ψ that really matter are c_0, c_2, and c_{-2}. For $r>0$, $|c_{2r}/c_0| \approx \mathcal{O}(q^{|r|}/4r^2)$. Thus, c_0 dominates over the other coefficients since $q \ll 1$. The particle trajectory is a low frequency sinusoid (both cosine and sine components) with frequency equal to ν, which is irrationally related to w in general (in our normalization $w=2$), and two low-amplitude high frequency components, of frequency $w+\nu$ and $w-\nu$, superimposed on that and other higher frequencies as can be seen from the expressions in Eqs. (6) and (7). The low frequency path is the one predicted by the ponderomotive force expression. To see this equivalence, we consider the ponderomotive force expression as given in Eq. (2). For the case when $g(x)$ corresponds to Eq. (1) with $p=0$, the ponderomotive equation for the low frequency path becomes

$$\frac{d^2x}{d\tau^2} = -\frac{1}{2}q^2x. \tag{13}$$

This has already been derived in the Introduction. The general solution to the above equation will be a linear combination of cos $\nu\tau$ and sin $\nu\tau$, where $\nu=q/\sqrt{2}$, which agrees with Eq. (10) for $p=0$. Thus, Eq. (13) is only approximate and the exact expression for ν is the asymptotic series given in Eq. (9) with $p=0$.

The expressions for v is

$$v = \frac{dx}{d\tau} = D\phi' + E\psi', \tag{14}$$

where $'$ represents differentiation with respect to τ. Putting $\tau=0$, in Eqs. (12) and (14), we get

$$\begin{aligned} x_0 &= D\phi_0 + E\psi_0, \\ v_0 &= D\phi_0' + E\psi_0', \end{aligned} \tag{15}$$

where the subscript 0 refers to the value of the corresponding functions at $\tau=0$. From Eqs. (6) and (7) it is clear that ϕ contains only cosine terms and ψ contains only sine terms. This means that ϕ' will contain only sine terms and ψ' will contain only cosine terms. Thus, $\phi_0'=0$ and $\psi_0=0$. Substituting this in Eq. (15), we solve for D and E, to get

$$\begin{aligned} D &= x_0/\phi_0, \\ E &= v_0/\psi_0'. \end{aligned} \tag{16}$$

Substituting this in Eqs. (12) and (14) and solving for x_0 and v_0, we obtain

$$\begin{aligned} x_0 &= \frac{1}{\psi_0'}(x\psi' - v\psi), \\ v_0 &= \frac{1}{\phi_0}(v\phi - x\phi'), \end{aligned} \tag{17}$$

where $\psi(\tau)$ and $\phi(\tau)$ are given by Eqs. (6) and (7). It is important to note that Eq. (17) is linear in x and v since ϕ and ψ are functions of time alone. Since $\phi_0\psi_0'$ is the nonzero Wronskian for Eq. (5), the denominators in Eq. (17) are strictly nonzero.

The distribution function of the plasma at any time τ can now be written as

$$f(x,v,\tau) = f_0[x_0(x,v,\tau), v_0(x,v,\tau)],$$

where $f_0(x_0,v_0)$ is the distribution function of the plasma at $\tau=0$. It must be noted that $f_0(x_0,v_0)$ can be any arbitrary function of x_0 and v_0.

III. TIME EVOLUTION OF THE DISTRIBUTION FUNCTION AND DENSITY

The time evolution of the distribution function and density of the plasma has a strong dependence on its expression at $\tau=0$. We consider a form of the initial distribution function given by

$$f_0(x_0,v_0) = n_0\sqrt{\frac{\beta_0}{2\pi}}\exp\left[-\beta_0\left(\frac{1}{2}v_0^2 + \gamma_0 x_0^2\right)\right], \tag{18}$$

where $\gamma_0>0$ is any non-negative real number which defines the scale length of the plasma for $\tau<0$, n_0 is the plasma density at $x_0=0$, and β_0 is a measure of the plasma temperature. We could have as well chosen any arbitrary distribution function, $f_0(x_0,v_0)$, instead of the Maxwellian, but we choose this since it is related to the idea of thermal equilibrium. For the above distribution function, the density of the plasma at $\tau=0$ is

$$n_0\exp(-\beta_0\gamma_0 x_0^2). \tag{19}$$

We have shown in Appendix A[41] that the analytic expression for the time evolution of the distribution function of the electrons is given by

$$f(x,v,\tau) = n_0\sqrt{\frac{\beta_0}{2\pi}}\exp\left[-\frac{\beta_0 a}{2\phi_0^2\psi_0'^2}\left(v-\frac{cx}{a}\right)^2\right]\times\exp\left(-\frac{\beta_0\gamma_0\phi_0^2\psi_0'^2}{a}x^2\right)$$

$$\Rightarrow f(x,v,\tau) = n_0\sqrt{\frac{\beta_0}{2\pi}}\exp\left\{-\frac{\beta_0}{2}\eta(\tau)[v-\xi(\tau)x]^2\right\}\times\exp\left[-\beta_0\gamma_0\frac{x^2}{\eta(\tau)}\right], \tag{20}$$

where

$$a(\tau) = \phi^2\psi_0'^2 + 2\gamma_0\psi^2\phi_0^2,$$

$$c(\tau) = \phi\phi'\psi_0'^2 + 2\gamma_0\psi\psi'\phi_0^2, \tag{21}$$

$$\eta(\tau) = \frac{\phi^2\psi_0'^2 + 2\gamma_0\phi_0^2\psi^2}{\phi_0^2\psi_0'^2},$$

$$\xi(\tau) = \frac{c(\tau)}{a(\tau)} = \frac{\phi\phi'\psi_0'^2 + 2\gamma_0\psi\psi'\phi_0^2}{\phi^2\psi_0'^2 + 2\gamma_0\psi^2\phi_0^2}, \tag{22}$$

and ϕ, ψ, ϕ_0, and ψ_0' were defined in the previous section. ϕ,ψ are purely functions of τ and ϕ_0,ψ_0' are nonzero constants. It should be noted that the method used in Appendix A[41] applies to arbitrary $f_0(x_0,v_0)$. We can now integrate Eq. (20) with respect to v to get the time evolution of the density of the plasma,

$$n(x,\tau) = n_0\exp\left(-\frac{\beta_0\gamma_0\phi_0^2\psi_0'^2}{\phi^2\psi_0'^2 + 2\gamma_0\psi^2\phi_0^2}x^2\right)\times\sqrt{\frac{\phi_0^2\psi_0'^2}{\phi^2\psi_0'^2 + 2\gamma_0\phi_0^2\psi^2}}$$

$$\Rightarrow n(x,\tau) = \frac{n_0}{\sqrt{\eta(\tau)}}\exp\left[-\beta_0\gamma_0\frac{x^2}{\eta(\tau)}\right], \tag{23}$$

$n(x,\tau)$ remains a Gaussian in x whose width fluctuates in time. This fluctuation has both high-frequency and low frequency components. It has been shown in Eq. (D9), Appendix D,[41] that for $q^2 \ll p \ll 1$,

$$\eta(\tau) = \frac{a}{\phi_0^2\psi_0'^2} = 1 + q\left[1+\frac{q}{4p}\right]\cos 2\nu\tau - q\cos 2\tau + \mathcal{O}(q^2).$$

This corresponds to the oscillation seen when an rf field of amplitude $2q$ is suddenly applied to a confined plasma at $\tau = 0$. It has been shown in Eq. (D4) that for $q \ll 1$,

$$\eta(\tau) = \frac{\gamma+\gamma_0}{\psi_0'^2}\left[1+\frac{\gamma-\gamma_0}{\gamma+\gamma_0}\cos(2\nu\tau) - q\cos(2\tau) + \mathcal{O}(q^2)\right],$$

where $[\beta_0\gamma_0]^{-1/2}$ is the scale-length of the initial plasma and $\gamma = \psi_0'^2/2\phi_0^2 \approx 0.5p + 0.25q^2$. For $\gamma = \gamma_0$, $\eta(\tau)$ becomes independent of ν. For general p,q, in Appendix B,[41] we show that for

$$\gamma \approx \frac{p}{2} + \frac{q^2}{4} \tag{24}$$

the functions $\xi(\tau)$ and $\eta(\tau)$ can be written as a Fourier series with fundamental frequency $w=2$. Also, $\xi(\tau)$ is purely a sine series and $\eta(\tau)$ is purely a cosine series, which can be written as

$$\xi(\tau) = \sum_{r=0}^{\infty} e_r \sin(2r\tau),$$

$$\eta(\tau) = \sum_{r=0}^{\infty} d_r \cos(2r\tau).$$

Thus, for this value of γ, the distribution function and density become

$$f(x,v,\tau) = n_0\sqrt{\frac{\beta_0}{2\pi}}\exp\left\{-\frac{\beta_0}{2}\sum_{r=0}^{\infty} d_r\cos(2r\tau)\times\left[v - x\sum_{r=0}^{\infty} e_r\sin(2r\tau)\right]^2\right\}\times\exp\left[-\frac{\beta_0\gamma}{\Sigma_{r=0}^{\infty} d_r\cos(2r\tau)}x^2\right] \tag{25}$$

and

$$n(x,\tau) = \frac{n_0}{\sqrt{\Sigma_{r=0}^{\infty} d_r\cos(2r\tau)}}\exp\left[-\frac{\beta_0\gamma}{\Sigma_{r=0}^{\infty} d_r\cos(2r\tau)}x^2\right]. \tag{26}$$

Thus, for $\gamma_0 = \gamma \approx 0.5p + 0.25q^2$, the time-varying terms in the distribution function and density have no dependence on ν and thus, the fluctuations in $f(x,v,\tau)$ and $n(x,\tau)$ are only a Fourier series with fundamental frequency w. This corresponds to a solution that is stationary in "slow time," one that oscillates at the rf frequency and its harmonics. This solution corresponds to an initial distribution that is invariant on curves of constant $E = 1/2v^2 + \gamma x^2$, which for $\gamma \simeq 0.5p + 0.25q^2$ confirms the "ponderomotive energy" concept for $p=0$. For the case of $p \neq 0$, this expression of γ can be viewed as a definition of the "generalized ponderomotive energy" concept where the particles see both the dc as well as the rf field.[1]

Although $\gamma \approx 0.5p + 0.25q^2$ corresponds to the usual notion of ponderomotive energy, this expression for γ is not quite exact. As is shown in Eq. (B11), Appendix B,[41] a more accurate expression for γ is

$$\gamma = \frac{1}{2}\left[\nu + \frac{2(c_2 - c_{-2})}{c_0 + c_2 + c_{-2}}\right]^2 = \frac{\nu^2}{2}[1 + 2q + \mathcal{O}(q^2)]. \tag{27}$$

For the case of $p=0$ and $q>0$, $\nu = q/\sqrt{2} + \mathcal{O}(q^3)$. Thus, for this case,

$$\gamma = \frac{q^2}{4}[1 + 2q + \mathcal{O}(q^2)]. \tag{28}$$

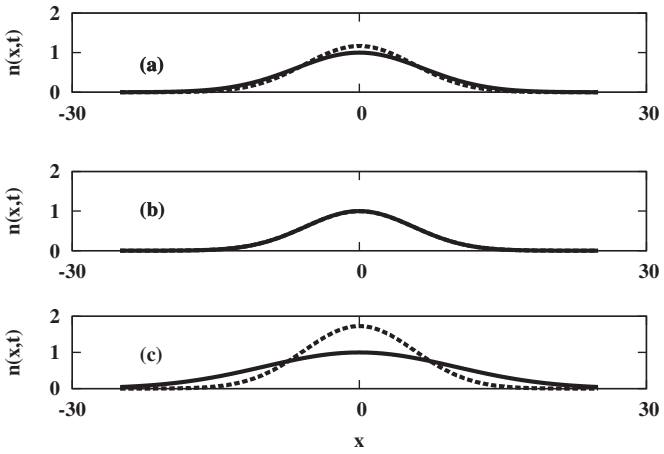

FIG. 3. This shows the density plots with $q=0.16$, $p=-0.01$ at two different times $\tau=0$ and $\tau=k\pi$, where $k\in N$ is such that $k\pi$ is close to $\pi/2\nu$. The three plots are for different values of γ_0. (a) $\gamma_0=0.5p+0.25q^2$; (b) $\gamma_0=\gamma$, where γ is given in Eq. (27); (c) $\gamma_0=20p+10q^2\gg\gamma$. In (a), it can be seen that the two curves are quite close to each other. This shows that, approximately, $\gamma=0.5p+0.25q^2$ is the value of γ_0 at which the density function does not have a large ν dependence. The curve in (b) clearly shows that Eq. (28) gives a much more accurate expression for the γ which leads to a more accurate expression for the ponderomotive energy of a particle under the linearly varying oscillatory electric field. The overlap of the curves at $\tau=0$ and $\tau=k\pi$ is so good that it is not visible in this graph. In (c) it can be clearly seen that for this value of γ_0, the density function has a strong dependence on ν.

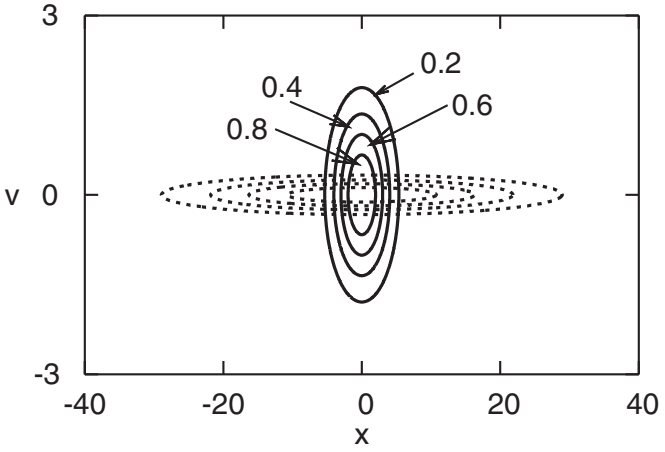

FIG. 4. This is the contour plot of the distribution function of the plasma for the case $\gamma_0=20p+10q^2$ with $q=0.16$, $p=-0.01$. The two superimposed contour plots correspond to the two times of the curves shown in Fig. 3(c). This clearly shows that the drastic change in the distribution function is the reason for the huge change in the density function over the ν time scale.

It has been numerically verified that the above expression for γ is much more accurate than $\gamma=0.25q^2$ and the second term in the brackets in Eq. (28) is of the order of q and is 0.3815 for $q=0.16$ and $p=0$. So, the improved expression for ponderomotive energy for the linear case when $p=0$ is

$$E=\frac{1}{2}v^2+\frac{q^2}{4}[1+2q+\mathcal{O}(q^2)]x^2. \tag{29}$$

Each of the three plots in Fig. 3 show two curves for the spatial variation of density corresponding to Eq. (23) at two different times $\tau=0$ and $\tau=2k\pi/\omega$. Here, $k\in N$ and is chosen such that $2k\pi/\omega$ is close to $\pi/(2\nu)$. These three plots are for three different values of γ_0, when $q=0.16$ and $p=-0.01$. Figure 3(a) is for $\gamma_0=0.5p+0.25q^2$, Fig. 3(b) is for $\gamma_0=\gamma$ as given by Eq. (27), and Fig. 3(c) is for $\gamma_0=20p+10q^2$. It can be seen in Fig. 3(a) that for $\gamma_0=0.5p+0.25q^2$, which corresponds to the conventional ponderomotive theory, the density is not absolutely invariant on the slow time scale. But if γ_0 is chosen according to Eq. (27), the density does not change on the slow time scale corresponding to frequency ν, which can be seen in Fig. 3(b). This confirms the accuracy of Eq. (27). Figure 3(c) shows that if γ_0 is arbitrarily chosen, then the density changes significantly on the slow time scale. This substantial change in density can be understood by considering the evolution of the distribution function in phase space which can be seen in Fig. 4. The density of particles at the turning points at $\tau=0$ is the density at $x=0$ at time $\tau\approx\pi/2\nu$. For arbitrary loading, this density differs from the density at $x=0$ at time $\tau=0$. This results in fluctuation of $f(x,v,\tau)$ at each point x, resulting in density fluctuations.

IV. SELF-CONSISTENT SOLUTIONS AND PLASMA CONFINEMENT

In the previous section, we have derived analytic expressions for the time evolution of the distribution function of a plasma under the electric field given by Eq. (1). The actual electric field in the plasma is given by

$$E(x,\tau)=E_e(x,\tau)+E_i(x,\tau),$$

where $E(x,\tau)$ is the total field given by Eq. (1), $E_e(x,\tau)$ is the externally applied electric field, and $E_i(x,\tau)$ is the self-field induced by the plasma electrons. $E_i(x,\tau)$ is given by

$$\frac{dE_i}{dx}=-4\pi en(x,\tau), \tag{30}$$

where $n(x,\tau)$ is the density of the electrons and the ions have been neglected since we are considering a pure electron plasma. The solution for the distribution function of the plasma obtained in the previous section is self-consistent if

$$E_e+E_i=-\frac{m}{e}[-B+A\cos(2\tau)]x$$

$$\Rightarrow E_e(x,\tau)=-\frac{m}{e}[-B+A\cos(2\tau)]x-E_i(x,\tau). \tag{31}$$

So, if an rf field is applied satisfying this equation, the plasma response becomes self-consistent. Equation (30) therefore becomes analogous to the nonlinear Poisson's equation in BGK mode theory. We repeat that this solution does not satisfy $\partial E/\partial x=4\pi\rho$. Thus, gradients of $\vec{E}$ must exist along y and z directions requiring some mechanism to keep particle motion along x.

If we excite the plasma with the above external field, then the $E_e(x,\tau)$ and $E_i(x,\tau)$ will add together to give an oscillating electric field, linearly varying in space, which can confine the plasma.

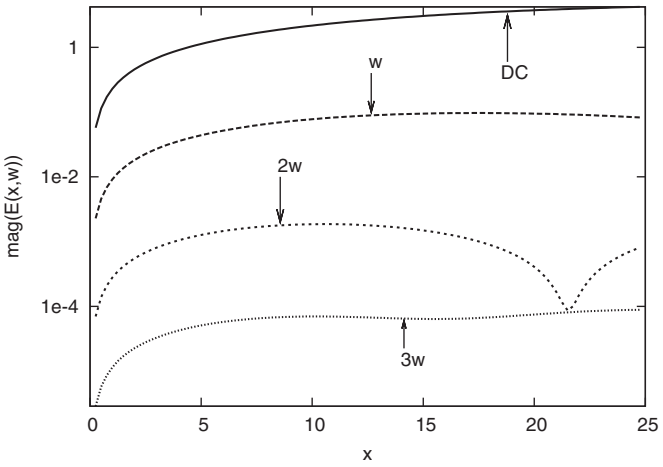

FIG. 5. This shows the spatial variation of the magnitude of various frequency components present in the Fourier transform of $E_i(x,t)$ as given by Eq. (32). This is for the case when γ is given by Eq. (27) and $q=0.16$, $p=-0.01$. As can be clearly seen, leaving the dc component, the component at ω is dominating. And we also have small contributions from components at frequencies 2ω, 3ω ($\omega=2$ in our normalization). The remaining harmonics are lower in magnitude than the ones shown. The component at 2ω is two orders of magnitude lower than that at ω. So, the field given by Eq. (32) is essentially a nonuniform monochromatic electric field for all practical purposes.

We have already shown in Eq. (23) that $n(x,\tau)$ is symmetric in x and is given by

$$n(x,t)=\frac{n_0}{\sqrt{\eta(\tau)}}\exp\left[-\beta_0\gamma_0\frac{x^2}{\eta(\tau)}\right],$$

where $\eta(\tau)$ is given by

$$\eta(\tau)=\frac{\phi^2\psi_0'^2+2\gamma_0\phi_0^2\psi^2}{\phi_0^2\psi_0'^2}.$$

Clearly, E_i is antisymmetric and hence is zero at $x=0$. Thus, the expression for E_i is

$$E_i(x,\tau)=\frac{-4\pi en_0}{\sqrt{\tilde{\eta}(\tau)}}\int_0^x\exp\left[-\beta_0\gamma_0\frac{x^2}{\tilde{\eta}(\tau)}\right]dx$$
$$=-2\pi en_0\sqrt{\frac{\pi}{\beta_0\gamma_0}}\,\mathrm{erf}\left[\sqrt{\beta_0\gamma_0}\frac{x}{\sqrt{\tilde{\eta}(\tau)}}\right],\qquad(32)$$

where erf is the error function. Thus, the right-hand side of Eq. (32) is fully specified for the given distribution function.

The Fourier components of the electric field, $E_i(x,\tau)$ are plotted in Fig. 5. As can be seen, the component at the rf frequency w dominates other higher harmonics. The difference between the components at w and $2w$ is two orders in magnitude.

Thus, only the fundamental and the bounce frequency components of $E_e(x,\tau)$ have significant amplitude,

$$E_e(x,\tau)=E_0(x)+E_\nu(x)\cos(\nu\tau)+E_1^+(x)\cos[(2+\nu)\tau]$$
$$+E_1^-(x)\cos[(2-\nu)\tau]+\cdots.$$

If γ_0 is such that Eq. (27) is satisfied, the ν dependence vanishes and for all practical purposes, $E_e(x,\tau)$ is a nonuniform monochromatic electric field with a dc component. For this value of γ_0, $\eta(\tau)$ is a cosine series and hence is a symmetric function of time and $E_e(x,\tau)$ becomes

$$E_e(x,\tau)=E_0(x)+E_1(x)\cos(2\tau).$$

Thus, when γ is given by Eq. (27), the Fourier decomposition of $E_e(x,\tau)$ is a pure cosine series and hence the component of $E_i(x,\tau)$ at frequency w is in phase with $E_t(x,\tau)$. Depending on the value of $-mB/e$ desired in Eq. (1), different $E_0(x)$ profiles are required.

V. DISCUSSION

A. The ponderomotive potential

The standard definition of the "ponderomotive potential" is based on first order theory. As a result, the value of ν is in error for larger field gradients. For electric fields linearly varying in space, the theory of Mathieu functions provides a better expression for the ponderomotive force, that includes the stability boundary. The expressions obtained in the previous sections describe exact solutions of the one-dimensional problem for the case of constant gradient fields. This is important since it permits us to validate theories in the literature against this exactly solvable case.

For the case of a linearly varying field, conventional ponderomotive force expressions approximately predict the low frequency path or the path along which the particle will drift. Based on this expression, the expression for the spatial variation of the time-averaged plasma density is derived. In two papers published in 1979, Krapchev and Abhay[20,21] showed that under the action of an electric field $-(m/e)wv_0(x)\cos(wt)$, the time-averaged density of the pure electron plasma will be $n=n_0\exp[v_0^2(x)/2v_T^2]$, where v_T is the thermal velocity of the plasma electrons. This is in agreement with the conventional ponderomotive theory. Krapchev's result, and indeed all of the conventional work, applies only to the $q\ll 1$ limit, as it is assumed that the gradients are weak.

When these expressions are applied to the field distribution studied in this paper, they predict that the time-averaged density should vary as

$$n=n_0e^{-\beta_0q^2x^2/4}.$$

From the expressions derived in this paper in Eq. (23), the actual instantaneous density is given by

$$n=\frac{n_0}{\sqrt{\eta(\tau)}}\exp\left[-\beta_0\gamma_0\frac{x^2}{\eta(\tau)}\right].$$

For $\gamma_0=\gamma$, the time-averaged expression for this density is given by [Eq. (C8), Appendix C[41]],

$$\overline{n(x)}=n_0\exp\left[-\frac{\beta_0}{2}\frac{q^2x^2}{2}\right]\left[1-\frac{q}{2}-\frac{\beta_0}{2}\frac{q^3x^2}{2}+\mathcal{O}(q^2)\right].\qquad(33)$$

While the exponential dependence is in agreement with ponderomotive theory, the additional multiplicative factors are not. These factors arise from the fact that the electron response is adiabatic and hence temperature is not a constant. In conventional ponderomotive theory, an implicit assump-

tion is made that the rf field is connected to a heat bath held at β_0. Hence this factor is not seen. However, such an assumption is questionable at rf frequencies. When the exact problem is solved, we find the additional factors. It is startling that there is a correction factor of $\mathcal{O}(q)$, which is a lower order than the ponderomotive effect itself. While this result has only been obtained for a very specific field profile, the source of the deviation from conventional theory suggests that a similar correction term would appear in any bounded system. Of course in the case of a linear gradient, this term is particularly significant, since the plasma response is exactly adiabatic at all collision frequencies, as is seen in the subsection discussion collisional response.

A question of interest is what changes are required in plasma fluid equations to obtain Eq. (33). The ponderomotive force is seen by all particles and as seen in Eqs. (6) and (7), the shape of the particle orbit is independent of the particle's initial conditions. Hence, on taking the moment, this force remains in its single particle form. However, as seen in Eq. (20), the temperature oscillates in "fast time" yielding a changed value for the average temperature as seen in Eq. (33). The equation of state therefore needs to be changed to $P=n\kappa\tilde{T}$, where fluid behavior is assumed to be isothermal. The time averaged temperature is [Eq. (C6), Appendix C[41]]

$$\tilde{T} = T_0[1 + q + \mathcal{O}(q^2)], \tag{34}$$

where $T_0=1/\kappa\beta_0$ is the initial temperature of the plasma. Substituting this into the momentum equation, the long term steady state density becomes

$$n = \tilde{n}_0 \exp\left[-\frac{\phi_P}{\kappa\tilde{T}}\right],$$

where ϕ_P is the ponderomotive potential energy of the each electron. The above expression for density is the well known Boltzmann relation. Since rf interaction preserves fluid, $\tilde{n}_0$ can be obtained from the initial conditions to yield

$$\overline{n(x)} = n_0\sqrt{\frac{T_0}{\tilde{T}}}\exp\left(-\frac{\phi_P}{\kappa\tilde{T}}\right).$$

Substituting $\phi_P=0.25q^2x^2(1+2q)$ from Eq. (29) and $\tilde{T}$ from Eq. (34), we obtain to first order

$$\begin{aligned}\overline{n(x)} &= n_0\sqrt{\frac{1}{1+q+\mathcal{O}(q^2)}} \\ &\quad\times\exp\left\{-\beta_0\frac{0.25q^2x^2[1+2q+\mathcal{O}(q^2)]}{1+q+\mathcal{O}(q^2)}\right\} \\ &= n_0\exp\left(-\frac{\beta_0}{2}\frac{q^2x^2}{2}\right)\left[1-\frac{q}{2}-\frac{\beta_0}{2}\frac{q^3x^2}{2}+\mathcal{O}(q^2)\right],\end{aligned} \tag{35}$$

which is in agreement with Eq. (33).

One difficulty with this modification of the fluid equations is that the solutions obtained in this paper exhibit adiabatic behavior for all rf frequencies and all collision frequencies. However, we conjecture that non idealities would relax the slow time behavior to make the isothermal equation of state, $P=n\kappa\tilde{T}$ valid.

In general, the exact plasma response also contains a term at the slow frequency, 2ν. This corresponds to the nonlinear, transient response. Conventional ponderomotive theory looks for steady state solutions, i.e., it assumes that the distribution function of the plasma can be expanded in a Fourier series which has the same fundamental frequency, w, as the applied field. However, unless γ is given by Eq. (27), a ν dependent term appears, and modifies the density perturbation. This is further discussed in the next subsections.

B. Relation to BGK theory

As can be seen in Fig. 5, the externally applied field *has a significant dc component*. This is the electric field that is required to balance the self-field induced by the plasma electrons. If we choose a value of γ for a particular p, q other than that given by Eq. (27), then the applied field will have components at frequency ν, in addition to a dc component and components at the rf frequency w and its harmonics. Existing treatments of this problem deal only with the field seen by particles, and thus neglect the need to balance this self-field.

The derivation in Sec. III was for a electron distribution function whose velocity variation was a Maxwellian. However, any arbitrary distribution could have been chosen that depended on x and v through $E_p=0.5v^2+\gamma_0x^2$. Let the distribution function of the plasma at $\tau=0$ be $f_0(x_0,v_0)=F(0.5v^2+\gamma_0x^2)$, where F is a smooth but otherwise arbitrary function of its argument. This distribution will evolve with time, and at an arbitrary time τ, it can be written as

$$f(x,v,\tau) = F\left\{\frac{\eta(\tau)}{2}[v-\xi(\tau)x]^2+\gamma_0\frac{x^2}{\eta(\tau)}\right\},$$

where $\eta(\tau)$ and $\xi(\tau)$ were defined in Eq. (22). The density of the plasma at any arbitrary time is thus

$$\begin{aligned}n(x,\tau) &= \int_{-\infty}^{\infty} f(x,v,\tau)dv \\ &= \int_{-\infty}^{\infty} F\left\{\frac{\tilde{\eta}(\tau)}{2}[v-\tilde{\xi}(\tau)x]^2+\gamma_0\frac{x^2}{\tilde{\eta}(\tau)}\right\}dv \\ &= \sqrt{\frac{1}{\tilde{\eta}(\tau)}}\int_{-\infty}^{\infty} F\left[\frac{u^2}{2}+\gamma_0\frac{x^2}{\tilde{\eta}(\tau)}\right]du,\end{aligned}$$

where

$$u = \sqrt{\tilde{\eta}(\tau)}[v-\tilde{\xi}(\tau)x] = \sqrt{\frac{1}{\tilde{\eta}(\tau)}}n\left[\sqrt{\frac{1}{\tilde{\beta}(\tau)}}x,\tau=0\right].$$

Corresponding to this density expression we can now find the induced field and, hence, the total external field required.

The same derivation shows that any such function of E_P yields a distribution that is time stationary with fluctuations at the rf frequency and its harmonics when γ is given by Eq.

(27). Each such distribution function corresponds to a different applied electric field. There is, thus, an interesting correspondence to BGK theory.

In the case of a BGK mode,[36] if we specify the electron distribution function as a function of energy, we can find the potential required to confine the plasma according to that particular distribution. If the distribution of the electrons is given by $f(E)$, this leads to the nonlinear Poisson's equation,

$$\frac{d^2\phi(x)}{dx^2} = 4\pi e \int_{-e\phi}^{\infty} \frac{f(E)dE}{\sqrt{2m[E+e\phi(x)]}}.$$

In this paper, we started with an initial distribution $f_0(0.5v_0^2 + \gamma x_0^2)$ at $\tau=0$. We assumed that the total field seen by the plasma must be $-(m/e)[-B+A\cos(wt)]x$. For this field, the particle paths are given by the Mathieu's functions. The distribution function and the density were obtained by the method given in Sec. III. From this we found the induced field,

$$E_i(x,t) = -4\pi e \int_0^x n(x',t)dx',$$

and hence, the total external field required to confine the plasma

$$E_e(x,\tau) = E_t(x,\tau) - E_i(x,\tau),$$

$E_e(x,\tau)$, and $f(E_P,\tau)$ constitute a self-consistent solution of the plasma evolution equations. There is a lack of consistency in the fact that $\partial E/\partial x \neq 4\pi\rho$. It requires that $\vec{E}$ vary along $\hat{y}$ or $\hat{z}$, yet the particles be constrained to move only along $\hat{x}$, perhaps by a magnetic field. For any given distribution of this form, we can determine the electric field that is to be imposed to make the problem self-consistent. The converse is, however, not possible. In general, $E_e(x,\tau)$ has an infinite number of harmonics, each of which has an independent spatial profile. Essentially what this means is that $E_e(x,\tau)$ can be an arbitrary function of time at each point in space. At most, $f(E_P,\tau)$ can match to one spatially varying harmonic of $E_e(x,\tau)$. Thus, for an arbitrary specification of $E_e(x,\tau)$, it is not possible to determine a distribution function that is invariant under the application of that field. The analogy with BGK theory is therefore limited.

The presence of plasma means that a dc field becomes present. This needs interpretation. BGK modes also correspond to time-stationary distributions that are confined by dc fields. If a dc field is also present here, what difference is there between the two?

The two types of solutions are clarified in Fig. 6. The figure shows the confining fields when a Maxwellian plasma is present. In order to compare, the static and the rf solutions are assumed to have the same time-averaged density profiles (Gaussian in shape). The static solution corresponding to a Maxwellian has a linear confining electric field (shown as the curve labeled "Effective static Field" in the figure). Charges execute simple harmonic motion in this field. The externally applied field is the difference of the desired linear field and the field induced by the charge density of the plasma. This is the curve labeled "Applied static Field" in Fig. 6. The self-consistent field itself is shown as the line labeled "Induced Field."

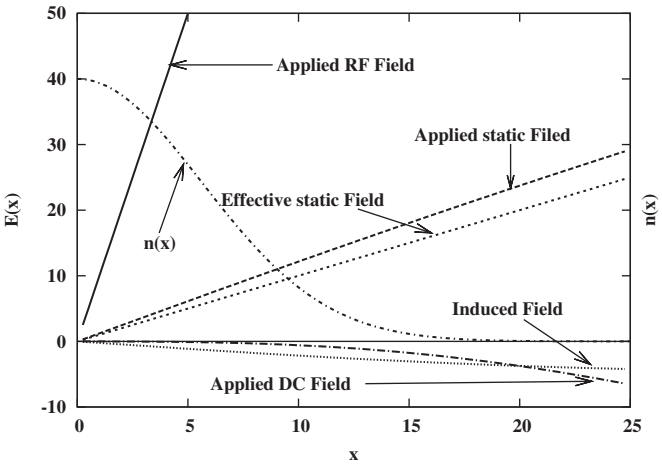

FIG. 6. This shows the relative spatial variation of the fields corresponding to the rf solution considered in this paper and the fields in static equilibrium. If the time-averaged density of the plasma goes like $\exp(-\beta_0\gamma_0 x^2)$, then the "Effective static Field" corresponds to the electric field for which the potential goes like $\beta_0\gamma_0 x^2$. The "Induced Field" is the field induced by the $\exp(-\beta_0\gamma_0 x^2)$ electron density in the absence of ions. The "Applied static Field" is the sum of these two fields, and is the external electric field which has to be applied to get this particular density profile. Now, if the same time averaged profile has to be achieved by using an rf field, then the total field seen by the plasma has a much steeper slope and is shown by the straight line labeled "Effective rf Field." The curves labeled "Induced Field" and "Applied static Field" are not straight lines. These curves are purely qualitative and are not to scale.

When rf is used to confine the plasma, the applied field is determined by the two parameters p and q. When q is zero (no rf), the resulting density corresponds exactly to the static solution above. When p is zero, the external applied field is assumed to have a dc component that exactly cancels the self-repulsion of the plasma. Then electrons see only an rf field, which is the case studied in Ponderomotive force studies in the literature. When both p and q are present, we have some very interesting possibilities. Figure 6 shows the case of $q=0.16$ and $p=-0.01$. The p value is assumed to be such that it corresponds exactly the self-repulsion of the plasma at $x=0$. At larger x there is a mismatch, since the self-field of the plasma grows as the error function while the total field is required to be linear. Thus an additional *repelling* field is necessary and is externally applied. This is shown as the negative dotted-dashed line in Fig. 6. For p that is more negative than this value, the dotted-dashed line will acquire a linear slope as well. For less negative p, a positive (confining) field develops that turns into a repelling field at greater distances.

The possibility of a repelling dc applied field is quite interesting. As is well known, static fields cannot confine charges. Thus, if perpendicular confinement is achieved electrostatically, parallel confinement must be achieved by other means such as rf. Yet, we see that a pure rf solution still requires a confining dc field which invalidates the solution. The solution to this problem is to use an extracting field along x. This ensures that the static field is consistent with

the averaging theorem of Laplace's equation. To confine the plasma along x, we apply an rf field that not only keeps the particles in via ponderomotive force, but also overcomes the dc repelling field that is present. Since there are small self-consistent contributions at the rf frequency and its harmonics, the applied field is slightly modified from $2qx\cos(2\tau)$. The rf field amplitude is shown as the nearly straight line labeled "Applied rf Field" in Fig. 6. The figure is only intended to convey the qualitative differences between static equilibrium and the rf solutions obtained in this paper, and is not to scale.

C. Collisional effects

The self-consistent solution we have obtained for the distribution function of the plasma has a Maxwellian velocity distribution at all spatial positions x and at all times τ. As is well known, the Maxwellian annihilates the point collision operator. Thus, the solution obtained in the previous section by solving the collisionless Vlasov equation is, in fact, a global thermal equilibrium. This shows that even in the presence of collisions, these solutions are still valid, because the system is already in the maximum entropy state by virtue of being described by a Maxwellian. This situation is quite different from that of a local thermal equilibrium where the distribution function is Maxwellian only to the lowest order. A distribution that is invariant to collisions can, obviously, not be subject to stochastic heating. This solution is therefore a solution where the plasma is confined by an rf field without undergoing heating.

If the plasma interaction is adiabatic, the temperature, T, and volume, V, of the plasma must satisfy the condition

$$TV^{C_p/C_v-1} = \text{constant},$$

where for a one-dimensional system $C_p/C_v=3$. The time evolution of the distribution function of the plasma is evaluated in Eq. (20) and found to be

$$\Rightarrow f(x,v,\tau) = n_0\sqrt{\frac{\beta_0}{2\pi}}\exp\left\{-\frac{\beta_0}{2}\eta(\tau)[v-\xi(\tau)x]^2\right\} \times\exp\left[-\beta_0\gamma_0\frac{x^2}{\eta(\tau)}\right].$$

From the above expression, we can see that $T\propto 1/\eta(\tau)$ and $V\propto\eta^{0.5}(\tau)$. Thus, $T\propto V^{-2}$. This gives

$$TV^{C_p/C_v-1}\propto V^{-2}V^{3-1} = \text{constant}.$$

The distribution function obtained in Eq. (20) clearly satisfies the adiabaticity condition.

Even more intriguing are the solutions for which γ is very different from the value given in Eq. (27). These are time-varying, exact solutions in which the plasma undergoes large-scale reorganization over the $\pi/2\nu$ time scale. These solutions also have Maxwellian velocity distributions *at all times and all spatial locations*! Thus, these time-varying solutions are also exact solutions of the one-dimensional, Vlasov–Boltzmann equation. Such solutions behave very similarly to the quasistatic compressions and rarefactions of ideal gases trapped in a piston, except that the compressions are not quasistatic, but happen at bounce times, and that the "walls" of the plasma piston are moving back and forth at rf frequencies (with harmonics at $r\omega\pm\nu$, $r=0,1,\ldots$). The breathing of the plasma at the bounce frequency ν is a self-consistent, exact response of the collisional plasma.

D. Multispecies plasmas

In this paper, we have considered a single species electron plasma. If we had ions in addition to electrons the problem changes somewhat. Each plasma species satisfies Eq. (1) with a different m_s/q_s ratio. Hence, Eq. (5) is satisfied by each species for p and q values that are scaled by m_s/q_s. The low frequency ν corresponding to the ions will therefore be different from that corresponding to the electrons. Nonetheless, a self-consistent, collisionless solution can be obtained, where

$$E_e(x,\tau) = -\frac{m}{e}[-B+A\cos 2\tau] - E_i(x,\tau),$$

where $E_i(x,\tau)$ is now the electric field induced by all the species present in the plasma. This solution will not however be invariant at the slow time. Each species has its own breathing frequency ν_s. By choosing q it is possible to eliminate the slow time variation of any one species, but the other species will continue to oscillate. However, for the special case of a two species plasma consisting of two oppositely charged species, it is possible to find p and q such that both species are time invariant at the slow time scale. Consider electrons and singly charged ions of mass m_i. Then,

$$\frac{p_e}{p_i} = \frac{q_e}{q_i} = -\frac{m_i}{m_e} = -k(\text{say}),$$

where $k\gg 1$. Now, we can approximately write γ from Eq. (23) as

$$\gamma = \frac{p_i}{2}+\frac{q_i^2}{4} = \frac{p_e}{2}+\frac{q_e^2}{4}$$

$$\Rightarrow p_i+\frac{1}{2}q_i^2 = -kp_i+\frac{1}{2}k^2q_i^2$$

$$\Rightarrow p_i(1+k) = \frac{1}{2}(k^2-1)q_i^2$$

$$\Rightarrow \frac{p_i}{q_i^2} = \frac{k-1}{2}.$$

For this choice of p and q, both the electron and ion distributions will be stationary in slow time.

Whatever the solution found, the presence of multiple species makes the solution susceptible to collisions. Clearly, when different species breathe at different frequencies, the distributions collisionally drag on each other. Even in the case where low frequency oscillations are eliminated for both species, the high frequency oscillations of ions and electrons are opposite in phase. This is obvious since the forces are opposite in direction. Hence there is a high frequency $v_i - v_e$ present, which means that collisional drag operates on these oscillations. Since these oscillations are driven by the

applied rf field, the collisional stability of such solutions and the possibility of collisionally driven heating of the distributions are issues that need investigation.

The special case of infinitely massive ions is interesting. The ion profile can be chosen to cancel the self-consistent field of the electrons. No dc confining field is now necessary (but is always permitted). The breathing solutions found are not collisionally valid, since the ions act as point scatterers that conserve energy but isotropize momentum. The stationary solutions are also collisionally invalid since the high frequency oscillations now see a momentum drag.

E. Linear response theory

Let us consider a situation when the total field seen by the plasma electrons is static for $\tau<0$, i.e., $E(x,\tau)=mpx/e$. At $\tau=0$, an rf field is switched on, and thus for $\tau>0$, $E(x,\tau)=-mx[-p+2q\cos(2\tau)]/e$ and the plasma behavior is governed by the analysis as given in this paper. If the rf field is very weak, the plasma response can be expected to obey the expressions given by linear theory.[37]

For $\tau<0$, the plasma is static and though the particles are moving around, the plasma density and distribution functions are independent of time,

$$f(x,v,\tau<0)=n_0\sqrt{\frac{\beta_0}{2\pi}}\exp\left[-\beta_0\left(\frac{1}{2}v^2+\frac{p}{2}x^2\right)\right]. \quad (36)$$

When the rf field is switched on, the plasma response will no longer be static but will evolve in time. As shown in the paper, the plasma response has two dominating frequency components, one at the rf frequency, $\omega=2$ and the other at the bounce frequency, 2ν, where ν is given by Eq. (10). In Appendix D,[41] it has been verified that the exact solutions obtained in the paper satisfy the linear Vlasov equation (for $q^2\ll p\ll 1$),

$$\frac{\partial f_1}{\partial t}+v\frac{\partial f_1}{\partial x}+\frac{-eE_0}{m}\frac{\partial f_1}{\partial v}+\frac{-eE_1}{m}\frac{\partial f_0}{\partial v}=0,$$
$$f_1(x,v,\tau)=f(x,v,\tau<0)(Av^2+Bx^2+Cxv), \quad (37)$$

where

$$A\approx-\frac{\beta_0}{2}[q\cos(2\nu\tau)-q\cos(2\tau)],$$
$$B\approx-0.5\beta_0 p[-q\cos(2\nu\tau)+q\cos(2\tau)], \quad (38)$$
$$C\approx\beta_0(-\sqrt{p}q\sin 2\nu\tau+q\sin 2\tau).$$

The linear limit corresponds to the rf field having an amplitude much smaller than the confining static field, i.e., $q\ll p$ (which automatically implies $q^2\ll p$). In this limit, Eq. (37) shows that not only is the response at ω linear in q, but so too is the response at 2ν.

Figure 7 shows the magnitude of the response at the two frequencies versus q at $x=0$. For $q\ll p$, the plasma oscillates with the same magnitude at both the high and the low frequency, even though the total electric field only contains a high frequency component. The solid thick line labeled $p=0.5q^2$ serves to divide two prominent regions of plasma response. To the left of this curve, the frequency components are more or less linear but after this region is crossed, the response becomes highly nonlinear. The curves shown in the figure are also in agreement with Eqs. (37) and (38). There is also another solid thick line on the curve labeled $p=0.25q$. This also demarcates two regions on the $p-q$ space. We can see that when q crosses this solid line, there is a visible change in the slope of the curves. Thus, as q becomes larger, the first nonlinearity to set in, is of the order of $q^2/4p$.

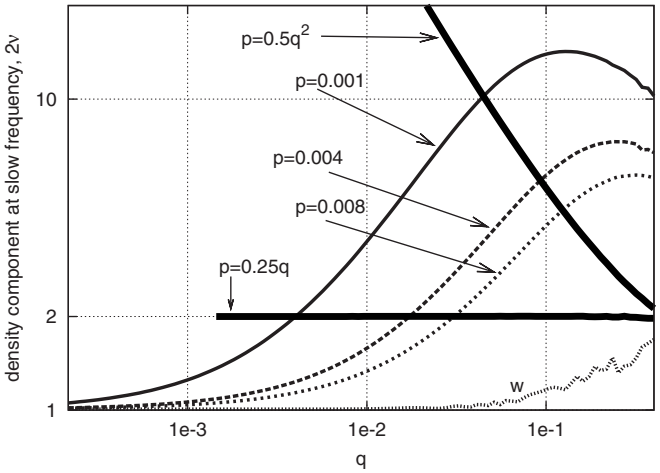

FIG. 7. This figure shows the plot of the magnitude of the coefficients of $\cos 2\nu\tau$ and $\cos 2\tau$ in the expression for A as given in Eq. (38), normalized by $0.5q$. It can be clearly seen that magnitude of the response at w lies below the response at 2ν. The solid thick line labeled $p=0.5q^2$ serves to divide two prominent regions of plasma response. When $p=0.5q^2$, the rf response is as large as the dc response and as we approach this region, plasma behavior is highly nonlinear. There is another solid thick line labeled $p=0.25q$. This also demarcates two regions in the $p-q$ space. As q crosses this line, there is a visible change in the slope of the curves. The plots clearly show that as q becomes large compared to p, the first nonlinearity to set in is of the order of $q^2/4p$. Also, the curves are well in agreement with the expressions derived in Eq. (37).

The electric field that is applied to the plasma is unbounded, since it is proportional to x. However, since the plasma's scale length is proportional to $1/\sqrt{p}$, the normalized magnitude of the rf field at the nominal edge of the plasma is $q\bar{x}=\mathcal{O}(q/\sqrt{p})\ll 1$. This perturbation is therefore an acceptable linear perturbation of a non-neutral plasma.

As shown above, the linear Vlasov theory is still valid. The response at 2ν represents the transient response. The rf field has been switched on at $t=0$. Thus, the plasma has experienced a small kick. The response at 2ν is due to this finite kick. But since $q\ll p$, the response at 2ν is still comparable in magnitude to the response at $\omega=2$. If $p\ll q$, then the plasma experiences a much harder kick and the response at 2ν will then be much larger than the response at $\omega=2$. In conventional wave theory, after linearizing the fluid equations, we do a Fourier transform to obtain steady state solutions. But the above results show that the Fourier transform must be done very carefully, because the transient response at frequencies other than the rf frequency may not die down to zero asymptotically.

F. Experimental realizability

It is not clear if the analysis carried out in this paper is realizable in practice. One can think of a plasma confined by a strong magnetic field along x that is subjected to an external rf field. However, the presence of plasma charges means that a curl-free electric field cannot achieve the desired confinement. This is so, since the total potential is required to be quadratic in x which limits the kind of density profiles that can be compensated. Suppose

$$\phi(x,\vec{r}_\perp,t) = C(\vec{r}_\perp,t)\frac{x^2}{2},$$

where $C(\vec{r}_\perp,t)$ is some function of its arguments. This implies

$$\nabla^2\phi = \frac{x^2}{2}\nabla_\perp^2 C(\vec{r}_\perp,t) + C(\vec{r}_\perp,t)$$

$$= 4\pi e n(x,\vec{r}_\perp,t)$$

$$\Rightarrow n(x,\vec{r}_\perp,t) = C_1(\vec{r}_\perp,t) + x^2 C_2(\vec{r}_\perp,t),$$

where the functions $C_1(\vec{r}_\perp,t)$ and $C_2(\vec{r}_\perp,t)$ depend on $C(\vec{r}_\perp,t)$. As the analysis in this paper shows, interesting plasma density profiles are Gaussian functions of x and hence do not fall into the above class of functions.

Possibly, a fully electromagnetic wave could compensate for a Gaussian density profile, but the authors have not been able to discover such an arrangement. The solutions in this paper are, therefore, presented as purely theoretical ideas.

VI. CONCLUSIONS

In this paper, we have obtained nonlinearly exact solutions for the one-dimensional rf confinement problem, for the case of spatially linear electric fields. The electric field considered is a combination of a dc field and an rf field, both of which vary linearly in space. Exact expressions for the distribution function and the particle density have been obtained in closed form. The assumption of a linear spatial dependence is very restrictive. However, it permits very strong results to be obtained. We find that single species plasmas confined in this field do not experience any stochastic heating. The solutions are valid even in the presence of strong collisions, where a Brownian motion or Fokker–Planck approach might be expected to yield more accurate results.

The nature of the ponderomotive force has been clarified to a certain extent in this study. Unless the plasma is already in a distribution of the form $f(E_P)$ when the rf field is turned on, the plasma response is not well approximated by the ponderomotive force equation. Instead, the plasma executes complex breathing cycles at a new frequency. The reason for this discrepancy in behavior lies in the implicit assumption of harmonic plasma ponderomotive response to an rf field. The plasma response to an rf field *is not in general harmonic*. Instead a bounce frequency appears, which is, in general, irrationally related to the rf frequency.

An implicit assumption made in the conventional theory of the ponderomotive effect[15,16] is that the nonuniform rf field does not effect the velocity space distribution of the plasma. But for the case of a linear field profile, we have found that this is not true. The temperature is found to oscillate on the rf time scales adiabatically and the time average of the temperature is found to depend on the rf field strength [Eq. (33)]. This is very significant and it is expected that deviations from conventional theory will be present for the case of spatially nonlinear rf fields also.

Among the surprising findings is a class of nonstationary solutions that do not relax in the presence of collisions. These are maximum entropy states that breathe at the electron bounce frequency. The plasma response shows spectral lines at $r\omega \pm k\nu$ for $r \in Z$ and $k=0,1,2$ and is not quasistatic by any definition of that term. Yet the solutions behave adiabatically in that they move from thermodynamic state to thermodynamic state along the isoentropic curves, in finite time.

The correction needed in fluid theory to account for the new terms in Eq. (33) were derived in Eq. (35). The derivation assumed that the fluid is isothermal under dc conditions. However, for the specific field profile studied in this paper, the fluid remains adiabatic even in dc conditions. We conjecture that nonlinear profiles would introduce sufficient mixing to drive the fluid to isothermal dc behavior, and that the case studied is not representative.

The main reason why the linear field problem yielded closed form solutions is also its weakness; all the particles in the plasma respond with the same frequency regardless of their initial position. Their orbits are not the same. However, fast and slow particles both respond identically. This is rather like a complex variant of simple harmonic motion.

When the field is spatially nonlinear, particle trajectories become much more complex. A single frequency no longer describes the electron bounce dynamics. However, numerical simulations still suggest that the orbits do not diverge and are still well described by $r\omega \pm k\nu$ for $r,k \in Z$. The difference is that ν is now not only a function of E_P, but also of the position along isoenergy curves. The analysis of plasma response in such fields is, of course, much more challenging.

The stability of both the time-independent and the time-dependent solutions obtained in this paper have yet to be determined and would shed light on the relaxation paths of these systems.

In this paper, we have considered only a monochromatic electric field. The case when many waves of different frequencies are present has also been considered in the past.[38–40] Turbulent growth of waves due to wave-wave interaction was shown to behave as diffusion in velocity-space in the quasilinear approximation. But it is beyond the scope of the present work to comment on this.

The Appendices of this paper are available at the EPAPS repository.[41]

[1] W. Paul, Rev. Mod. Phys. **62**, 531 (1990).
[2] R. Breun, S. N. Golovato, L. Yujiri, B. McVey, A. Molvik, D. Smatlak, R. S. Post, D. K. Smith, and N. Hershkowitz, Phys. Rev. Lett. **47**, 1833 (1981).
[3] C. F. Shelby and A. J. Hatch, Phys. Rev. Lett. **29**, 834 (1972).
[4] A. J. Hatch and J. L. Shohet, Phys. Fluids **17**, 232 (1974).
[5] R. B. Hall and R. A. Gerwin, Phys. Rev. A **3**, 1151 (1971).

[6]S. Ikezawa, S. Yamamoto, and S. Takeda, J. Phys. Soc. Jpn. **53**, 2529 (1984).
[7]P. H. Probert, Ph.D. thesis, University of Wisconsin-Madison, Dissertation Abstracts International, Vol. 46-04, Sec. B, p. 1215 (1985).
[8]J. L. Shohet, Ann. N.Y. Acad. Sci. **251**, 94 (1975).
[9]I. Siemers, R. Blatt, Th. Sauter, and W. Neuhauser, Phys. Rev. A **38**, 5121 (1988).
[10]C. G. Goedde, A. J. Lichtenberg, and M. A. Lieberman, J. Appl. Phys. **64**, 4375 (1988).
[11]M. A. Lieberman and V. A. Godyak, IEEE Trans. Plasma Sci. **26**, 955 (1998).
[12]P. Wood Blake and M. A. Lieberman, IEEE Trans. Plasma Sci. **23**, 89 (1995).
[13]M. A. Lieberman and A. J. Lichtenberg, Phys. Rev. A **5**, 1852 (1988).
[14]E. Fermi, Phys. Rev. **75**, 1169 (1949).
[15]R. W. Gould, Phys. Lett. **11**, 236 (1964).
[16]H. A. Blevin, J. A. Reynolds, and P. C. Thonemann, Phys. Fluids **13**, 1259 (1970).
[17]H. A. Blevin, J. A. Reynolds, and P. C. Thonemann, Phys. Fluids **16**, 82 (1973).
[18]M. A. Lieberman, IEEE Trans. Plasma Sci. **16**, 638 (1988).
[19]O. A. Popov and V. A. Godyak, J. Appl. Phys. **57**, 53 (1985).
[20]V. B. Krapchev, Phys. Rev. Lett. **42**, 497 (1979).
[21]V. B. Krapchev and A. K. Ram, Phys. Rev. A **22**, 1229 (1980).
[22]J. Cary and A. Kaufman, Phys. Rev. Lett. **39**, 402 (1977).
[23]C. Grebogi, A. N. Kaufman, and R. G. Littlejohn, Phys. Rev. Lett. **43**, 1668 (1979).
[24]J. Slepian, Proc. Natl. Acad. Sci. U.S.A. **36**, 485 (1950).
[25]H. A. H. Boot, Nature (London) **30**, 1187 (1957).
[26]D. R. Nicholson, *Introduction to Plasma Theory* (Wiley, New York, 1983), p. 31.
[27]R. R. Birss, Phys. Educ. **4**, 33 (1969).
[28]J. R. Cary and A. N. Kaufman, Phys. Fluids **24**, 1238 (1981).
[29]C. Grebogi and R. G. Littlejohn, Phys. Fluids **27**, 1996 (1984).
[30]G. J. Morales and Y. C. Lee, Phys. Rev. Lett. **33**, 1016 (1974).
[31]B. M. Lamb and G. J. Morales, Phys. Fluids **26**, 3488 (1983).
[32]E. Mathieu, Jour. de Math. Pures et Appliquees (Jour. de Liouville) **13**, 137 (1868).
[33]J. Y. Hsu, K. Matsuda, M. S. Chu, and T. H. Jensen, Phys. Rev. Lett. **43**, 203 (1979).
[34]N. W. McLachlan, *Theory and Applications of Mathieu Functions* (Oxford University Press, Oxford, 1947), p. 20.
[35]A. Abramowitz and A. Stegun, *Handbook of Mathematical Functions* (Dover, New York, 1964), p. 722.
[36]I. B. Bernstein, J. M. Greene, and M. D. Kruskal, Phys. Rev. **108**, 546 (1957).
[37]R. C. Davidson, H-W. Chan, C. Chen, and S. Lund, Rev. Mod. Phys. **63**, 341 (1991).
[38]W. E. Drummond, Phys. Fluids **7**, 816 (1964).
[39]R. E. Aamodt and M. C. Vella, Phys. Rev. Lett. **39**, 1273 (1977).
[40]S. Hans, Phys. Rev. Lett. **42**, 1339 (1979).
[41]See EPAPS Document No. E-PHPAEN-15-059805 for Appendices A–D. For more information on EPAPS, see http://www.aip.org/pubservs/epaps.html